Ultrathin Au-alloy Nanowires at the Liquid-Liquid Interface

Dipanwita Chatterjee[1], Shwetha Shetty A.[1], Knut Müller-Caspary[2], Tim Grieb[2], F.F. Krause[2], Marco Schowalter[2], Andreas Rosenauer[2] and N. Ravishankar[1]*

1. Materials Research Centre, Indian Institute of Science, Bangalore 560012

2. University of Bremen, Otto-Hahn-Allee NW1, D-28359 Bremen

Table of Content:

Experimental Section:

Materials required:

Gold Chloride ($HAuCl_4.xH_2O$) from Kem Light Laboratories Pvt. Ltd., Copper chloride dehydrate ($CuCl_2.2H_2O$) extrapure from SD Fine-Chem Limited (SDFCL), Hexa Chloro Palladate (IV) (K_2PdCl_6) from Sigma Aldrich, Hexa Chloro Platinic Acid ($H_2PtCl_6.xH_2O$) from Kem Light Laboratories Pvt. Ltd, AR grade Ethylene glycol from SDFCL, AR grade extrapure Dextrose (D-Glucose) from Sisco Research Laboratories Pvt. Ltd., oleylamine from Sigma Aldrich, LR grade oleic acid from SDFCL, Triisopropyl silane (TIPS) from Sigma Aldrich, AR grade Hexane from SDFCL were obtained. Standard Pt/C (40%) and Pd/C (10%) were acquired from Sigma-Aldrich.

Synthesis method:

Au nanowire template: 3 mg of $HAuCl_4.xH_2O$, 3 ml hexane and 100 μlit of oleylamine were taken in a centrifuge tube and sonicated at room temperature until the Au precursor dissolves completely. After cooling the reaction mixture down to room temperature 150 μlit of TIPS was added and the reaction mixture was finally homogenized and left undisturbed for 24 hrs. After 24 hrs Au nanowire was observed to precipitate at the bottom of the centrifuge tube. The product was centrifuged at 2000 rpm for 15 mins, the supernatant was discarded and the precipitate was used for the next step.

AuCu nanowire synthesis: Considering Au precursor has completely converted to Au nanowire and been separated by centrifugation 1.3 mg of $CuCl_2.H_2O$ was dissolved in 4 ml ethylene glycol (EG) in a 10 ml microwave vial to maintain 1:1 molar ratio with Au. 200 μlit of Oleic acid was added to the above solution, sonicated until the salt was completely dissolved and left for a while for the polar (EG) layer to separate from the nonpolar (oleic acid) layer. Oleic acid coordinates with Cu^{2+} and extracts it to the nonpolar layer (evident from the green coloured nonpolar layer in optical image, fig S1 (b)). Oleic acid also prevents oxidation of metallic Cu to its oxides[1, 2]. 10 mg of glucose (considering 1 mole

of electron transfer from 1mole of glucose) was added as a reducing agent for Cu to the mixture and it got dissolved in the ethylene glycol layer. The centrifuged and separated Au nanowire was dissolved in 1ml hexane and 200 μlit of oleylamine and was transferred completely to the reaction mixture in the microwave vial. Au nanowire solution in hexane being nonpolar floats at the top portion of the reaction mixture in the lighter non polar part. This separation prevents the Au wire from breaking during reaction as polar medium accelerates the breaking kinetics of Au nanowire. The microwave vial is subjected to microwave heating conditions maintained at 100^{o}C for a hold time of 25 mins, then 110^{o}C for 25 mins, 120^{o}C for 15 mins and 130^{o}C for 15 mins sequentially at a power limit of 25 Watt and pressure limit of 100 psi.

AuPd nanowire synthesis: 3.2 mg of K_2PdCl_4, 10 mg of glucose and 200 μlit of oleylamine were added to 4 ml of EG in 10 ml microwave vial and sonicated until the Pd precursor completely dissolves. Pale yellow translucent solution of Pd^{+2} ions-coordinated with oleylamine forms on the top (Optical image, fig S1 (c)) of which Au nanowire solution in hexane and 200 μlit oleylamine is transferred as before and microwave reaction was done under the above mentioned condition.

AuPt nanowire synthesis: 3.1 mg of $H_2PtCl_6.xH_2O$ and 200 μlit of oleylamine were mixed with 4 ml of EG in a 10 ml microwave vial and sonicated until complete dissolution of Pt precursor. When left to settle after sonication oleylamine coordinated with $[PtCl_6]^{+2}$ ions extracts Pt^{+4} ions to the nonpolar layer and floats atop EG as a separate nonpolar layer (yellow in colour, as shown in optical image, Fig S1 (d)). 10 mg of glucose was added which dissolved in the EG layer. Au nanowire in hexane and 200 μlit oleylamine is transferred to the vial as before and the vial was subjected to microwave reaction conditions as mentioned before.

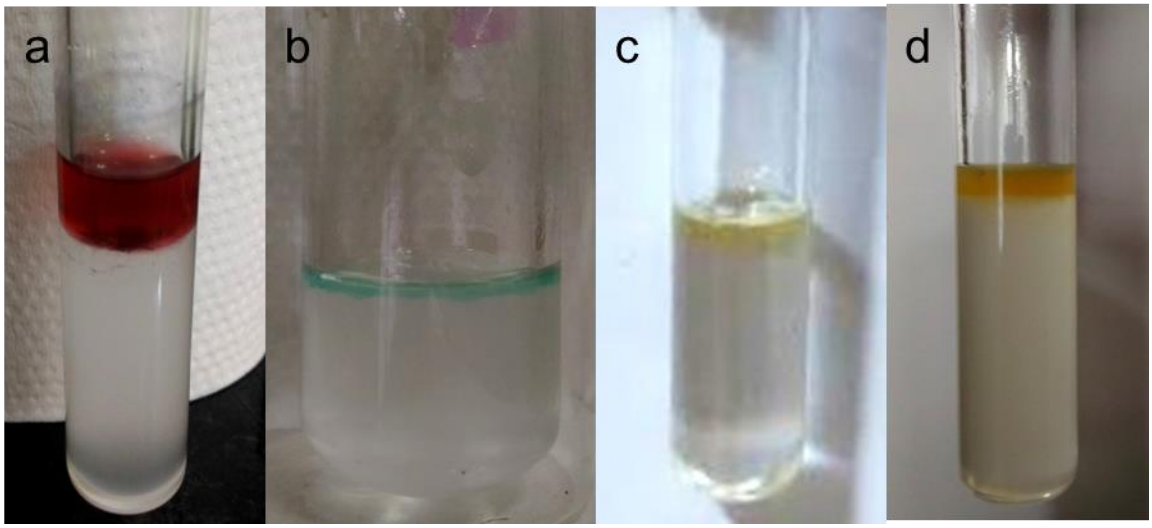

Figure S1: Optical images nonpolar-polar interface in case of template Au nanowires in hexane-oleylamine on the top and EG at the bottom in (a), Cu salt-oleic acid complex on the top and EG at the bottom in (b), Pd-salt-oleylamine complex on the top and EG at the bottom in (c) and Pt salt-oleylamine complex on the top and EG at the bottom in (d).

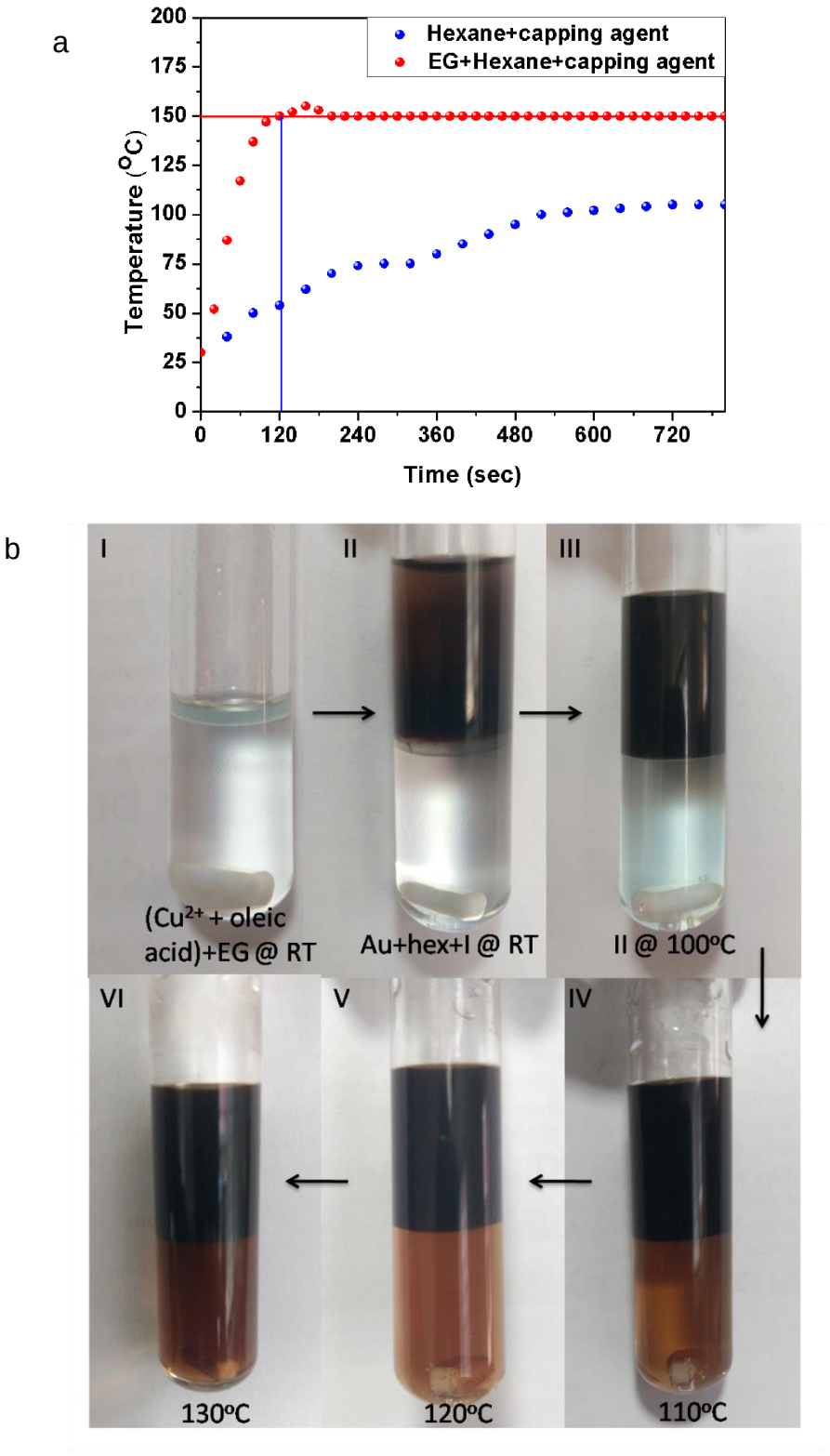

Figure S2: Temperature vs time profile of microwave heating is shown in (a). The set temperature was 150°C. EG being a high loss solvent absorbs heat more steeply and reaches 150°C (the reaction temperature) in about 2mins. Hexane being a nonpolar solvent, having zero loss, cannot absorb microwave radiation to get heated. Still the temperature is shown to rise slowly due to slow heating of the microwave vessel (Silica). However, the temperature becomes steady after reaching about 100°C. (b) shows a temperature dependent change in the colour of the reaction system in different stages.

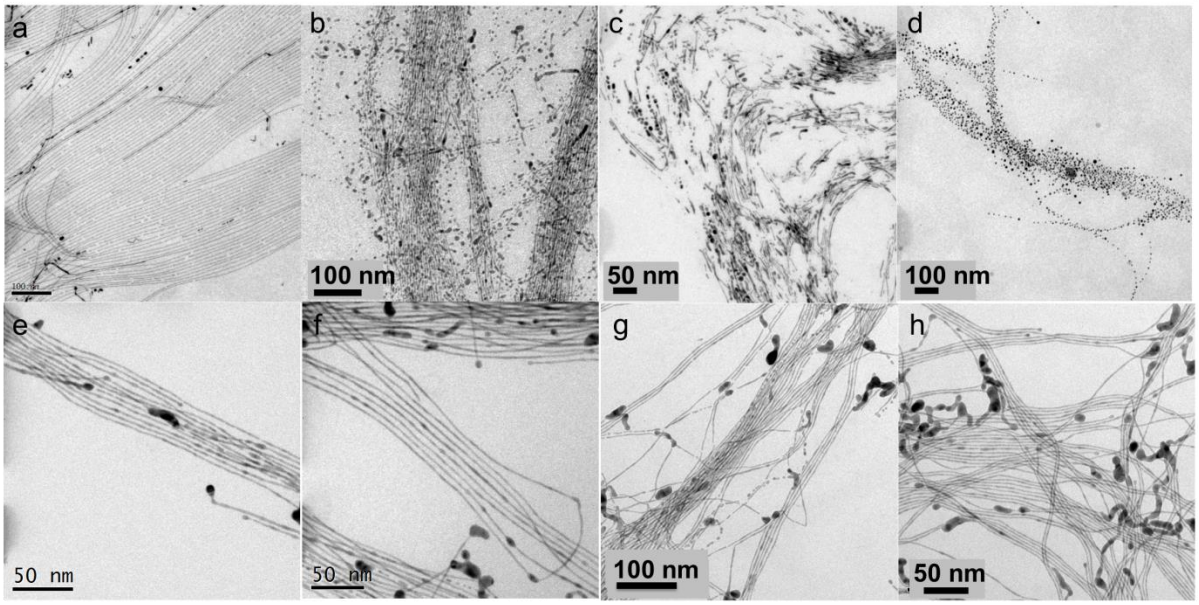

Figure S3: (a) As synthesized Au nanowires washed in hexane medium at room temperature, (b) sample after alloy wire formation reaction done only in EG without the two layer (nonpolar-polar) configuration keeping rest of the other conditions constant, demonstrating that the wires are not intact, (c) Pristine Au wires after keeping in ethanol medium (polar) for an hour and the wires seem to break, (d) Pristine Au wires broken into particles due to heating at 150^{o}C for 1hr in furnace demonstrating the unstable nature of the wires, (e) and (f) are images of AuPd and AuPt wires respectively after heating at 200^{o}C for 1 hr, (g) and (h) are images of AuPd and AuPt nanowires respectively after being sonicated in Ethanol for 1hr demonstrating the robustness of the wires.

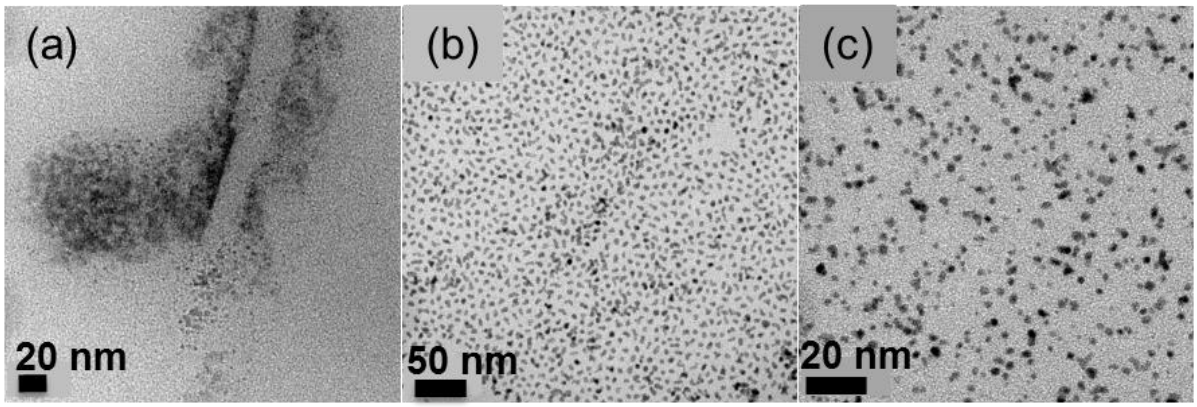

Figure S4: Bright field low magnification TEM images of reduced of $CuCl_2$, K_2PdCl_6 and H_2PtCl_6 without Au nanowire template under the same reaction conditions as alloy wire synthesis is shown in (a), (b) and (c) respectively. ~3 nm Pd and Pt particles are seen to form in images (b) and (c) respectively, whereas reduction of Cu precursor remains incomplete (evident from the color of the solution after reaction). Hence wire formation not seen without the template.

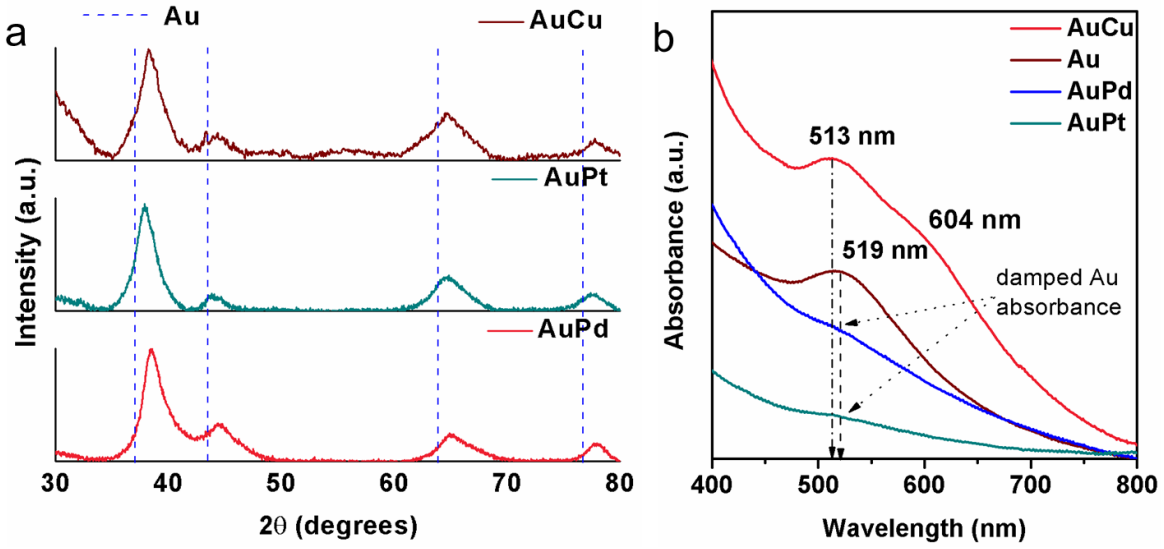

Figure S5. (a) X-ray diffraction pattern of Au (shown in blue dotted line), AuCu, AuPd and AuPt shows shift of Au peaks in all the alloys confirming alloy formation. The crystal structure conforms to FCC. (b) UV-Visible spectrum of Au, AuCu, AuPd and AuPt nanowire samples.

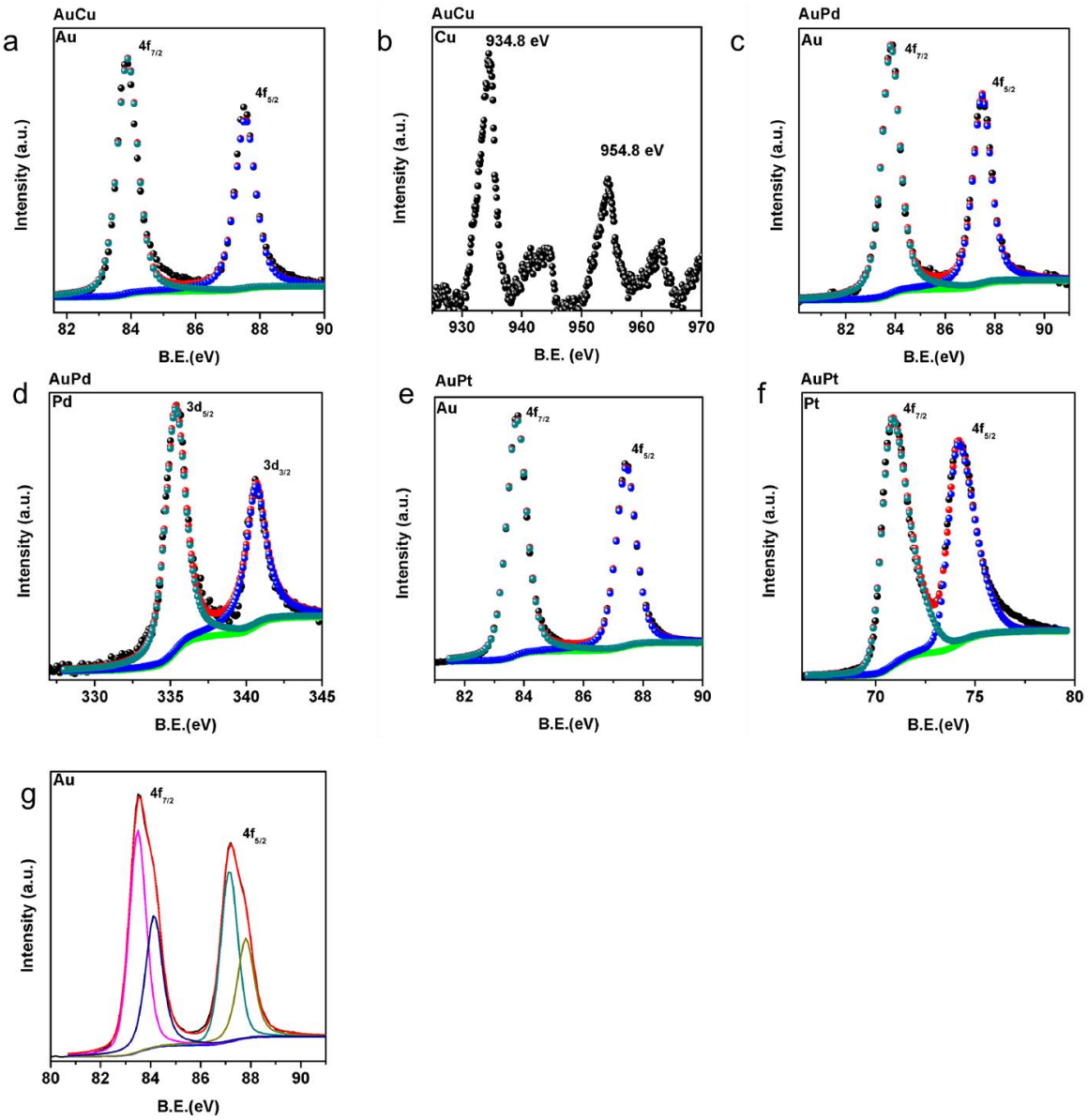

Figure S6. X-ray Photoelectron Spectrum of Au and Cu in AuCu alloy wires in (a) and (b) respectively, Au and Pd in AuPd alloy nanowires in (c) and (d) respectively, Au and Pt in AuPt alloy nanowires in (e) and (f) respectively and pristine Au nanowires in (g)

Table S1. Analysis of XPS data:

Sample	Element	Peak	Peak position (ev)
AuCu wires	Au(0)	$4f_{5/2}$	87.547
		$4f_{7/2}$	83.895
	Cu	$2p_{1/2}$	954.8
		$2p_{3/2}$	934.8
AuPd wires	Au(0)	$4f_{5/2}$	87.293
		$4f_{7/2}$	83.620
	Pd(0)	$3d_{3/2}$	340.460
		$3d_{5/2}$	335.145
AuPt wires	Au(0)	$4f_{5/2}$	87.436
		$4f_{7/2}$	83.762
	Pt(0)	$4f_{5/2}$	74.150
		$4f_{7/2}$	70.828
Au wires	Au(0)	$4f_{5/2}$	87.34
		$4f_{7/2}$	83.68
	Au^{+1}	$4f_{5/2}$	88.00
		$4f_{7/2}$	84.33

XPS measurement was done to get information about the valence states of the component elements of the metal alloy nanowires. All the alloy nanowires have XPS signal from both its constituent elements and tabulated in SI, table S1 indicating presence of both the metals in the wires. From the binding energy (B.E.) values it is evident that Au, Pd and Pt are present in their zero valent states. For Cu, shake up and shake off peaks are observed which indicate presence of surface oxides along with Cu(0)[3]. For AuPd with alloying there is no shift in the peak for Au or Pd with respect to pure components, only increase in width occurs due to inter diffusion of Au in Pd[4].

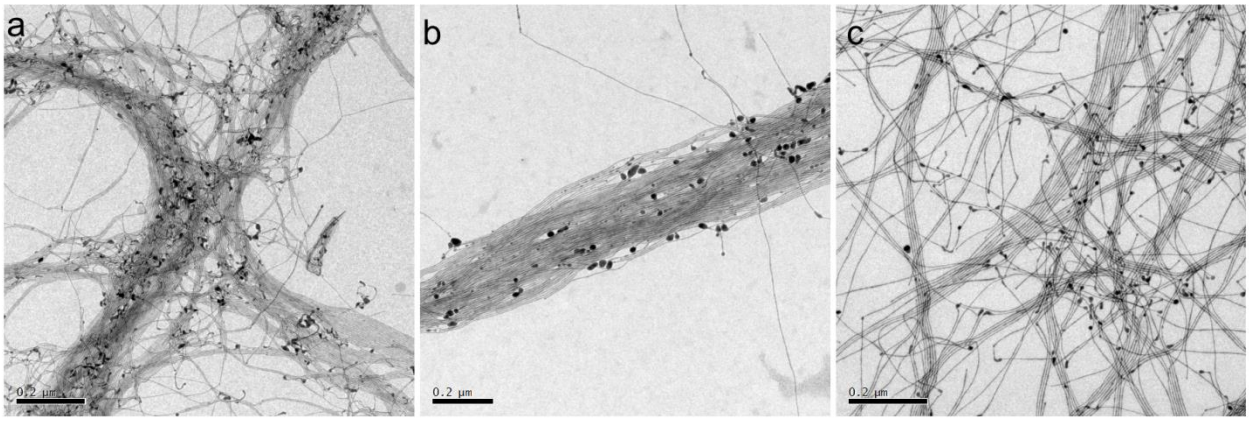

Figure S7: Low magnification images of AuCu (a), AuPd (b) and AuPt (c) wires showing that the wires are long and ultrathin.

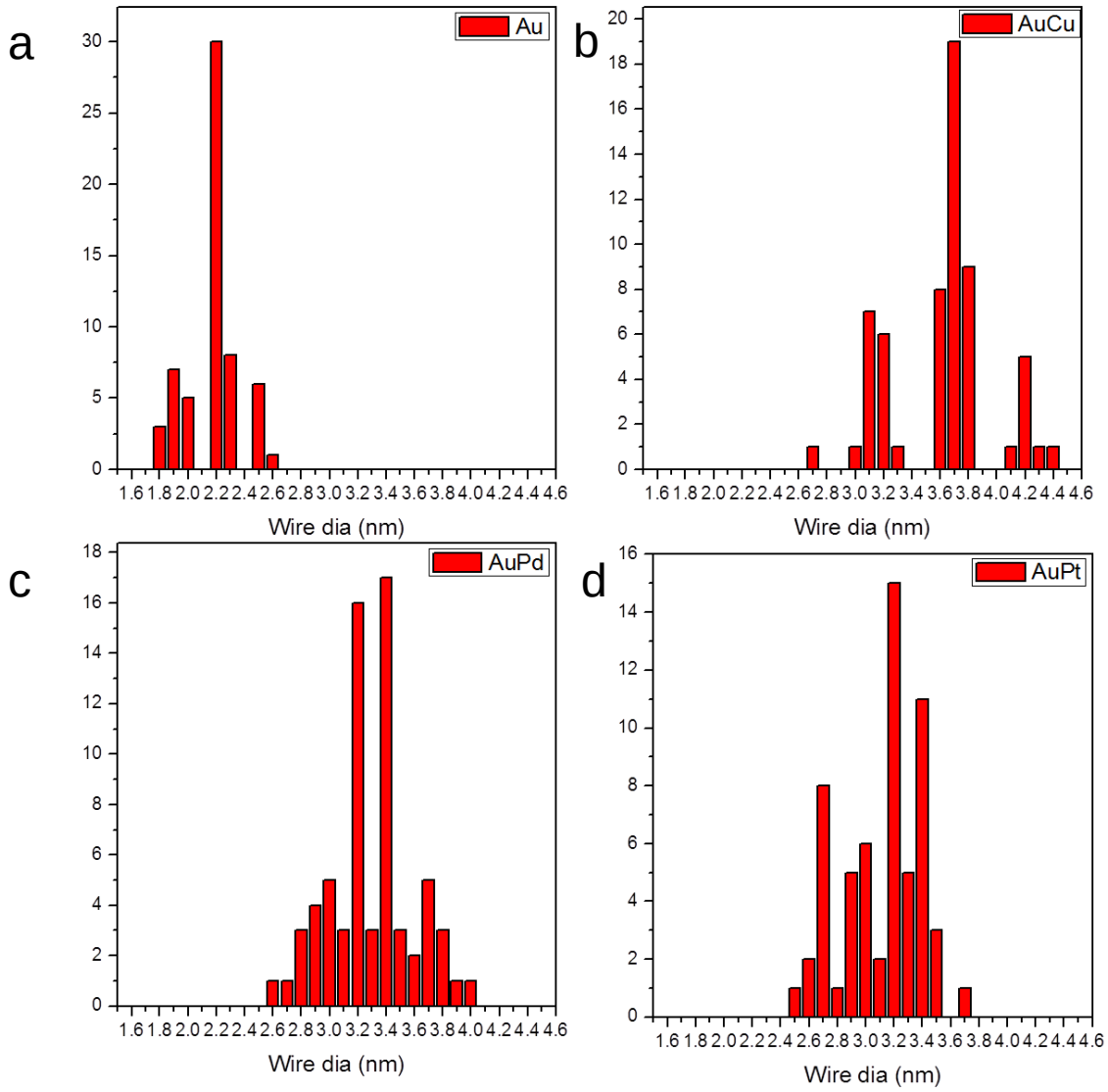

Figure S8: Histogram of dia of Au, AuCu, AuPd and AuPt wires showing a shift in the thickness of the alloy nanowires towards 3.6nm compared to 2nm thick Au nanowires.

The increase in thickness accounts for the percentage of additional metal (M) added. The percentage of M is calculated from EDS. The calculations are given as follows.

If we assume a wire with a hexagonal cross section as shown below, addition of successive shells of the second metal M leads to an increase in the diameter of the wires. We have calculated the diameter increase and the corresponding change in the composition of the wires as listed in the table below.

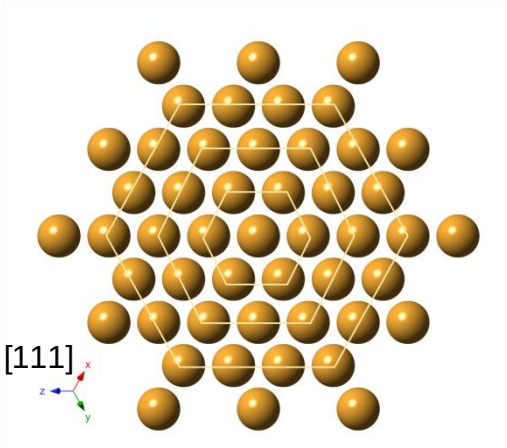

Representative cross section of the wire. Each shell marked in light yellow hexagon

Shell number (n)	Total no. of atoms (S_n)	No. of atoms in n^{th} shell (a_n)
0	1	1
1	7	6
2	19	12
3	37	18
4	61	24
5	91	30
6	127	36

Number of atoms in consecutive shells, starting from shell number (n) = 1 goes as 6, 12, 18, 24 … in an arithmetic progression with a common difference (d) 6.
The no. of atoms in n^{th} shell can be counted as $a_n = a_1 + (n-1)d$
The total number of atoms in the wire till shell n is $S_n = 1 + n/2\ [2a_1 + (n-1)d]$
Calculating distance between two nearest neighbour atoms in the [110] direction we find that wire diameter of 2 nm corresponds to about shell number n=4 and wire diameter of 3.6 nm corresponds to about n=6. We have calculated the percentage of M with respect to (wrt) total atoms (T) and also wrt pure Au in the following table hypothetically considering addition of M in the 5^{th} shell and 6^{th} shell.

n	Number of Au atoms	Number of M atoms added	Total atoms (T)	% of M atoms wrt T
5	61	30	91	33
6	61	66	127	52

Considering the wire diameter extends up to n=5 and shell of M in n=6 the percentage of M wrt T and pure Au are given below.

n	Au atoms	M atoms	Total atoms (T)	% of M atoms wrt T	% of M atoms wrt pure Au
6	91	36	127	28	39

The above table indicates that the addition of 1 or 2 shells to the existing wire of ~ 2 nm diameter leads to a composition of ~ 30-50% that is consistent with the experimental observations.

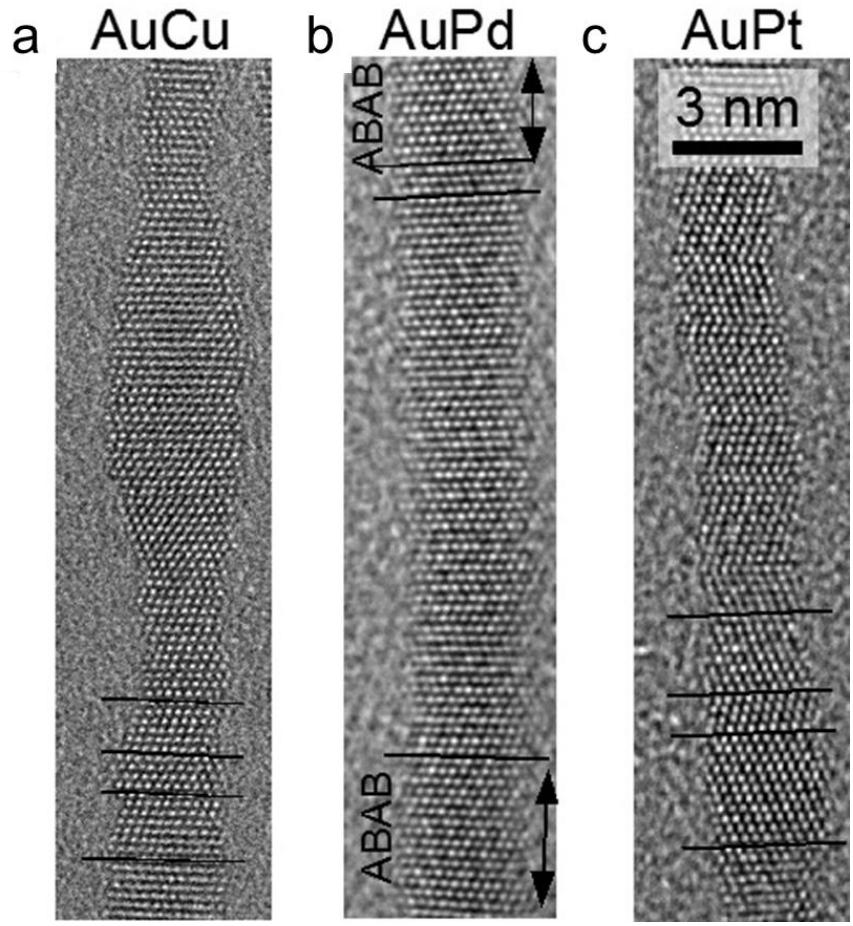

Figure S9: (a)-(c) High resolution transmission electron microscopy (TEM) images of AuCu, AuPd and AuPt alloy nanowires revealing a large number of twin boundaries. (Some are indicated by black lines.) For the AuPd system additionally regions with a hexagonal stacking as well as stacking faults were observed.

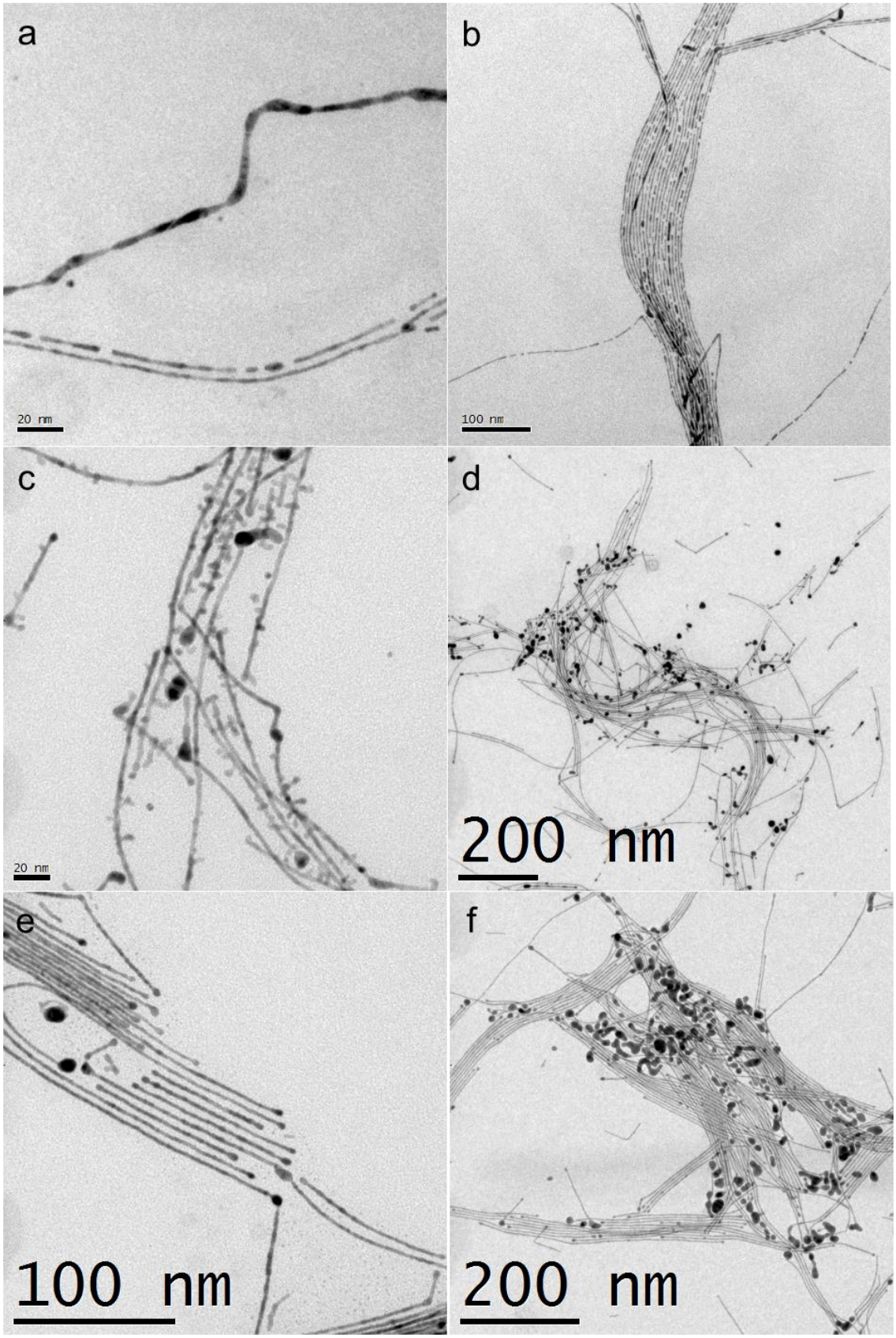

Figure S10. Different compositions of AuM alloy nanowires obtained by varying the percentage of the M precursor: Low magnification images of (a) $AuCu_3$, (b) Au_3Cu, (c) $AuPd_3$, (d) Au_3Pd, (e) $AuPt_3$ and (f) Au_3Pt alloy nanowires

Electron microscope conditions:

A FEI Tecnai F30 microscope, operated at 300 kV acceleration voltage has been used for low mag and high resolution imaging and a FEI Titan G2 60-300 microscope, operated at acceleration voltage of 300 kV, spot size 6 has been used for STEM-EDS mapping . High resolution images for defect study were taken in a FEI Titan 80-300 microscope equipped with a correction system for the spherical aberration of the objective lens at an acceleration voltage of 300 kV.

For quantitative analysis of EDS Cu K lines and L lines for Au, Pd and Pt were considered.

Electrochemical Measurements:

Electrochemical measurements were carried out in a conventional 3 electrode electrochemical set up connected to a potentiostat (Model PG-16250, Techno Science Instruments, Bangalore). Platinum foil and saturated Ag/AgCl electrode served as counter and reference electrodes respectively. To prepare the working electrode freshly synthesized AuPd/ AuPt nanowires are dispersed in 2mL hexane solution mixed with 100uL of ethanol and 20uL of 5%w/w Nafion solution (Alfa Aesar) and sonicated well for 5min. This catalyst ink is drop casted on a fixed geometrical area on a strip of Toray carbon paper electrode and air dried. Weight of the catalyst is 0.5mg. Commercial Pt/C (40%) and Pd/C (10%) catalyst electrodes are used for comparison. To prepare the catalyst ink, 3mg of the dry catalyst powder is dissolved in 1 ml of ethanol mixed with 20uL of 5% w/w Nafion solution and sonicated for 5min and dropcasted on Toray electrode of fixed geometrical area. The weight of Pt/C and Pd/C catalyst is 1.7 mg and 1.8 mg respectively. The geometrical area of the catalyst is kept constant at 0.5 cm^2.

Cyclic voltammetry (CV) scans for the measurement of electrochemical surface area (ECSA) were performed in Ar saturated 0.5M KOH solution bath. Initial set of 10 cycles performed prior to get a reproducible data for all the samples. ECSA for AuPt and Pt/C are calculated by standard procedure of integrating the area under the anodic desorption peak for the under potentially deposited hydrogen after double layer charge correction (Q_H in cm^2). Specific ECSA is calculated using the formula $Q_H/0.21xM_{Pt}$ where M_{Pt} is the loading of the active metal Pt in AuPt or Pt/C (in mg/cm^2) and 0.21 is the charge due to the complete oxidation of a monolayer of adsorbed hydrogen on pure Pt surface (in mC/cm^2). For AuPd and Pd/C electrodes, ECSA is determined from the standard procedure of integrating the area under the cathodic Pd-O reduction peak (Q_O in cm^2). Specific ECSA is calculated using the formula $Q_O/0.42xM_{Pd}$ where M_{Pd} is the loading of the active metal Pd in AuPd or Pd/C(in mg/cm^2) and 0.42 is the charge due to the reduction of a monolayer of oxide layer on the surface of pure Pd surface (in mC/cm^2).

CV studies for methanol oxidation reaction (MOR) were carried out in 0.5 M KOH and 1 M methanol electrolyte bath solution at a scan rate of 40 mV/sec and the currents are normalized with respect to ECSA and loading mass of active metal Pt/Pd (main paper, Fig.4 a-d).

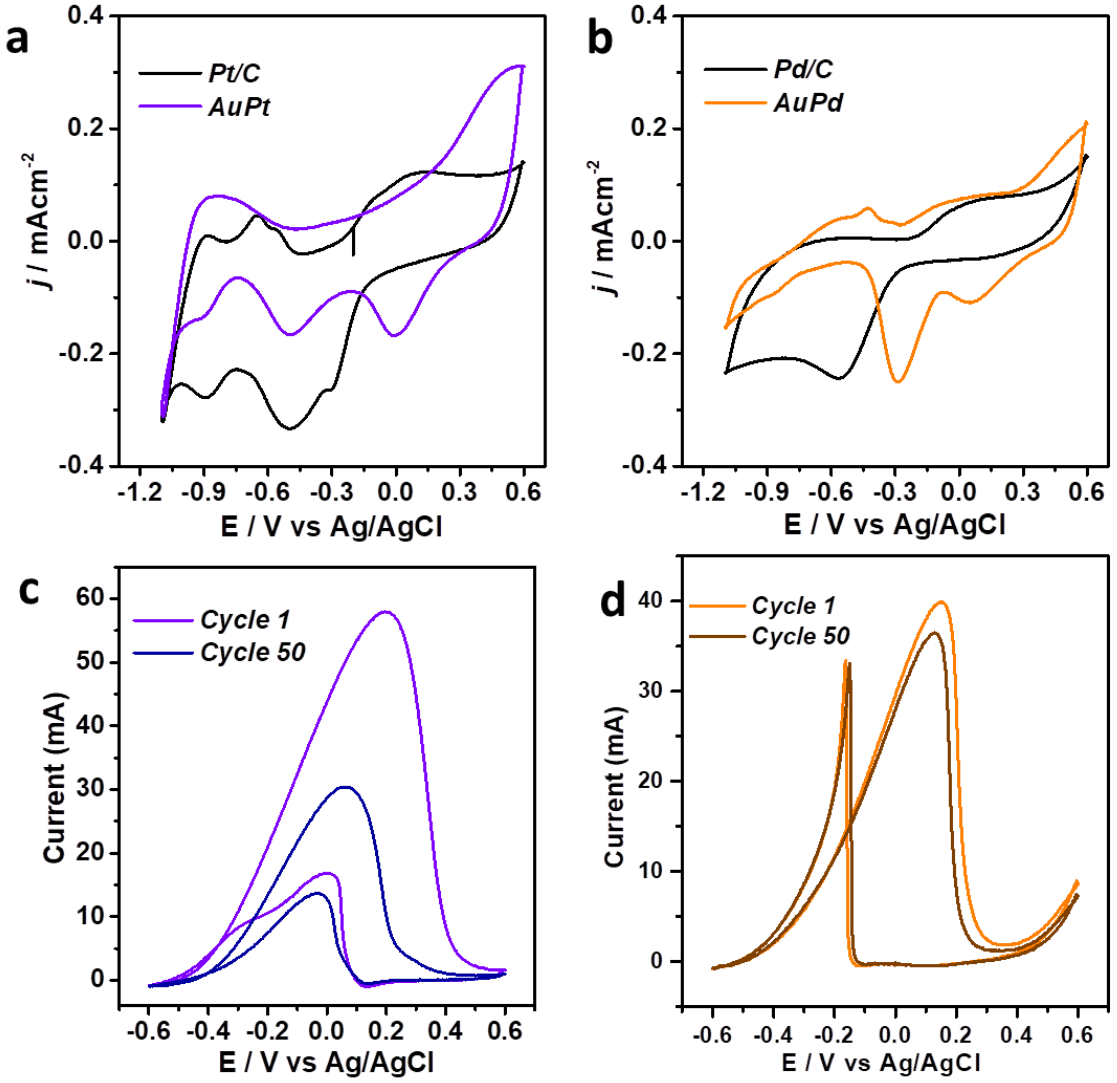

Figure. S11: (a) and (b) CV curves for AuPt, Pt/C, AuPd and Pd/C for ECSA measurements in Ar saturated 0.5M KOH solution at a scan rate of 40mV/S. (c) and (d) CV curves for methanol oxidation at a scan rate of 20mV/S for AuPt and AuPd electrodes. The first CV cycle and 50th cycle are displayed here to understand the durability of respective catalysts towards methanol oxidation. AuPt shows 50% degradation in current whereas AuPd shows about 10% loss in activity at the end of 50th cycle.

Specific ECSA values are 23.8, 24.8, 11.9 and 56.6 m^2/g for AuPt, AuPd, Pt/C and Pd/C respectively in alkaline medium.

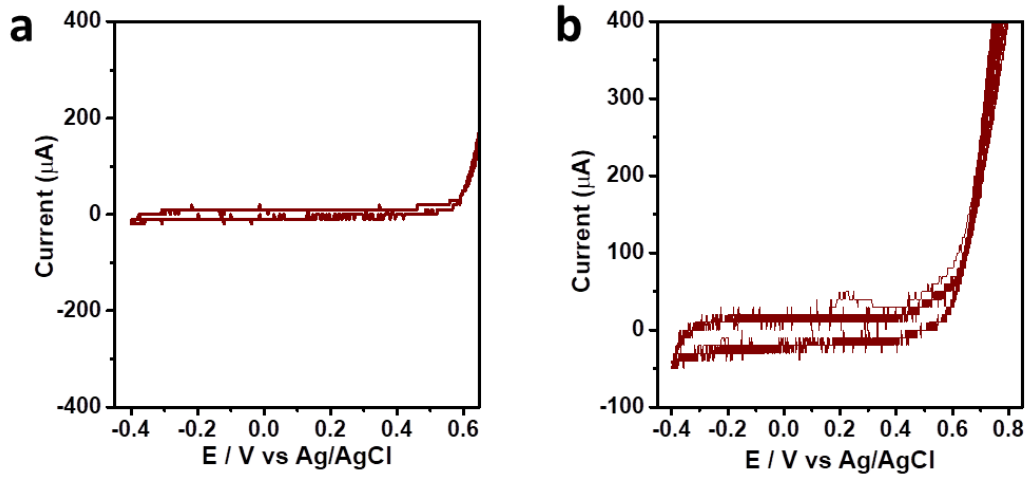

Figure. S12: CV curves for Au nanowires (a) in Ar saturated 0.5M KOH solution at a scan rate of 40mV/S (b) methanol oxidation in 0.5M KOH + 1M methanol solution at a scan rate of 100mV/sec. Current values are negligible < 100μA in both the studies. AuPt and AuPd wires show currents of the order of magnitude 2 compared to that of Au NWs.

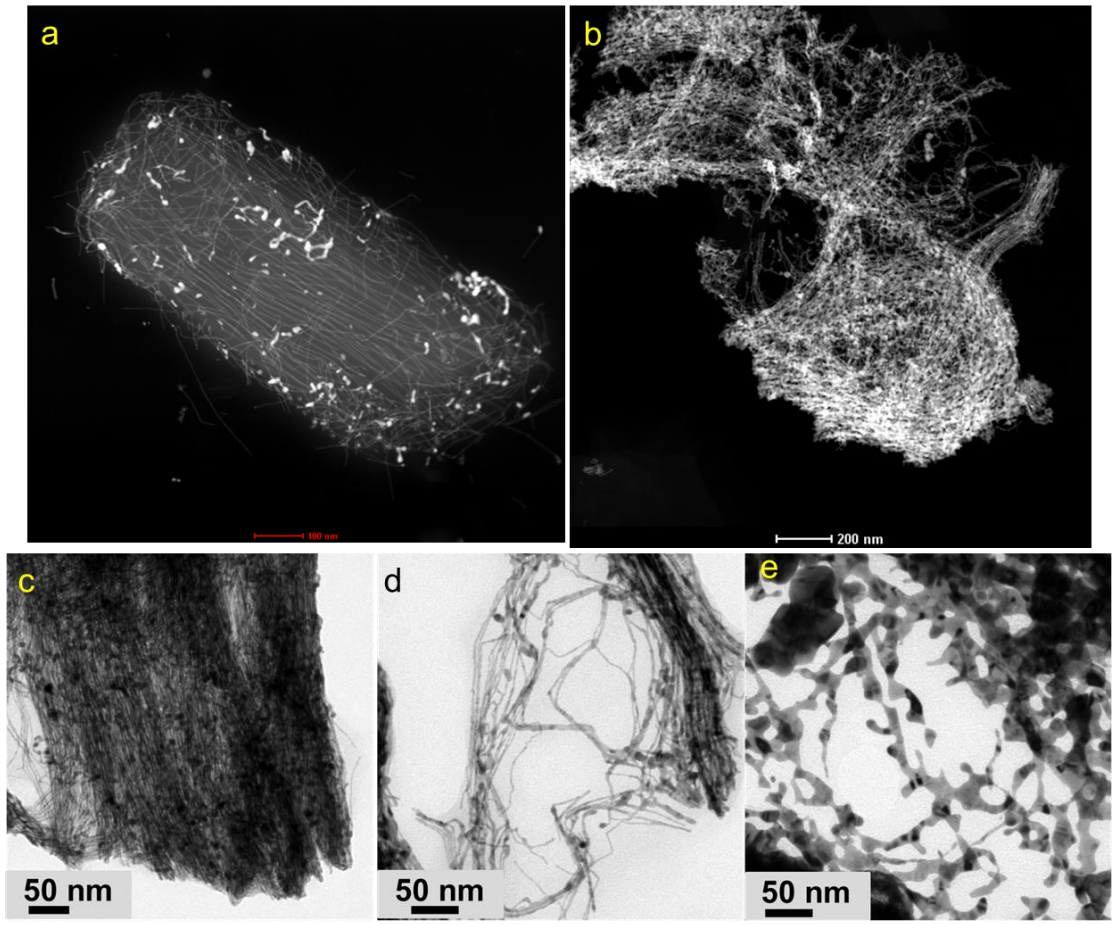

Figure S13. (a) and (b) are HAADF-STEM images of AuPd and AuPt nanowires scraped out from the electrodes after 60 cycles of MOR, (c)-(e) Evolution of AuPt nanowire morphology with increasing number of cycles from 5 via 10 to 60 respectively.

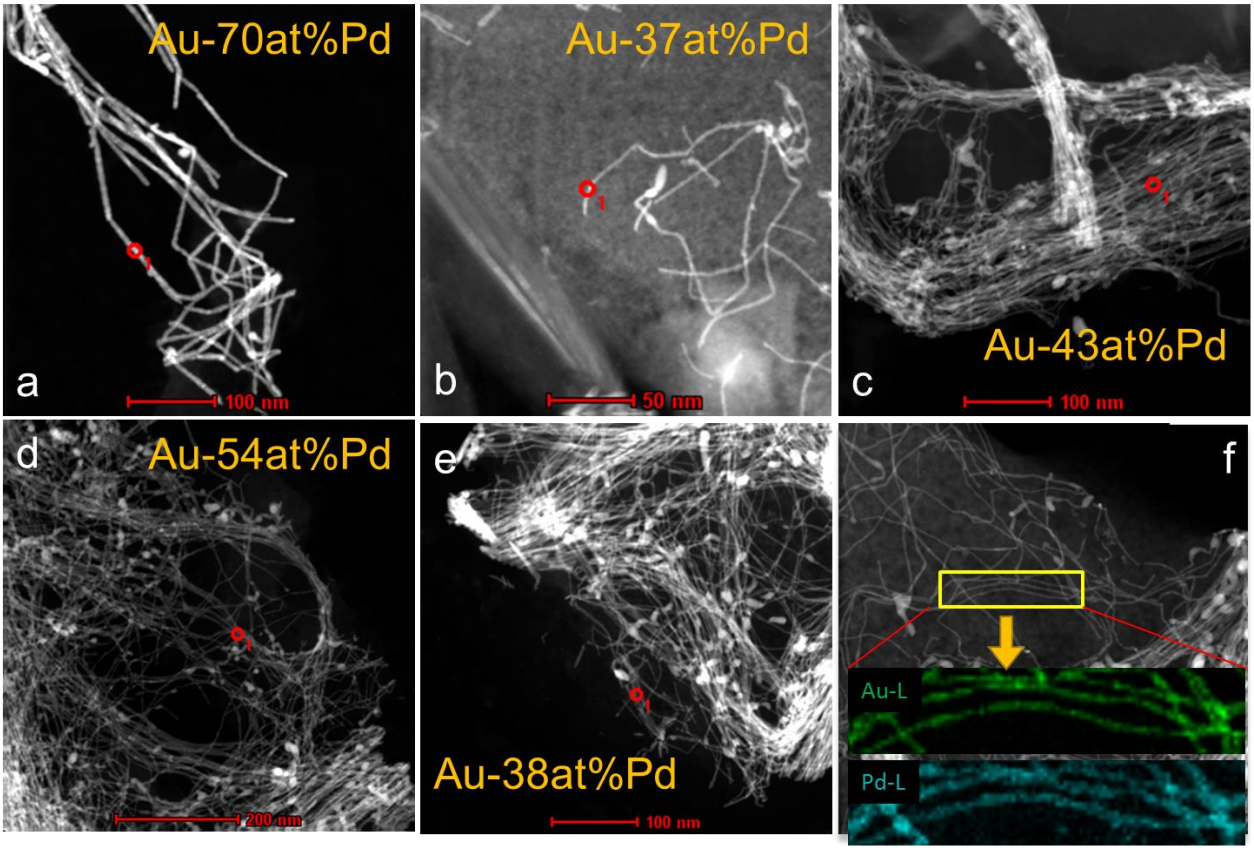

Figure S14. (a-e) shows quantified point EDS from representative 5 regions showing variation of Pd percentage from 70% - 40%. The wire morphology is retained all over. (f) shows HAADF-STEM EDS mapping from a representative area of the sample showing presence of Au and Pd all over along the length of the wire.

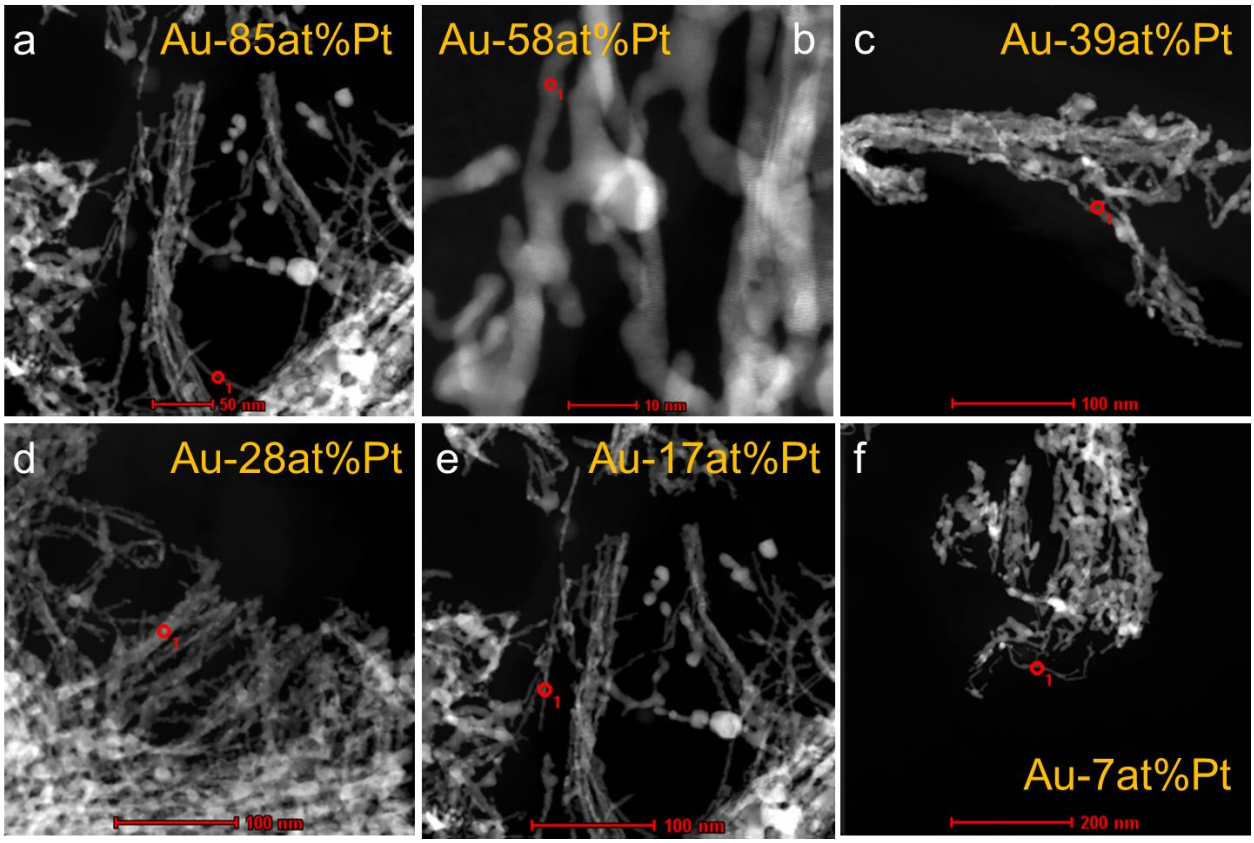

Figure S15. (a-f) shows quantified point EDS from 6 different regions and percentage of Pt has changed over a much larger range unlike the sample before catalysis, where average composition was Au-40%Pt.

Table S2: Composition of AuPt and AuPd before and after catalysis

Sample	Average Composition (before catalysis)	Average Composition (after catalysis)
AuPt	Au-30.2(±10.2)at%Pt	Au-39(±23.5)at%Pt
AuPd	Au-32.8(±5.5)at%Pd	Au-35.4(±4.4)at%Pd

References:

1. Yang, J.-g.; Zhou, Y.-l.; Okamoto, T.; Bessho, T.; Satake, S.; Ichino, R.; Okido, M. *Chem. Lett.* **2006,** 35, (10), 1190-1191.
2. Jeong, S.; Lee, S. H.; Jo, Y.; Lee, S. S.; Seo, Y.-H.; Ahn, B. W.; Kim, G.; Jang, G.-E.; Park, J.-U.; Ryu, B.-H. *J. Mater. Chem. C* **2013,** 1, (15), 2704-2710.
3. Huang, S.-S.; Liu, L.; Mei, L.-P.; Zhou, J.-Y.; Guo, F.-Y.; Wang, A.-J.; Feng, J.-J. *Microchim. Acta* **2016,** 183, (2), 791-797.
4. Koel, B.; Sellidj, A.; Paffett, M. *Phys. Rev. B* **1992,** 46, (12), 7846.